The Effects of Dielectric Shield on Specific Absorption Rate and Heat Transfer in the Human Body Exposed to Microwave Energy

Teerapot Wessapan*, Siramate Srisawatdhisukul and Phadungsak Rattanadecho

Department of Mechanical Engineering, Faculty of Engineering, Thammasat University,
Klong Luang, Pathumthani, 12121, Thailand

*Corresponding Author: teerapot@yahoo.com, Tel (02) 564-3001-9, Fax (02) 564-3010

Abstract

This paper proposes a numerical study to simulate the effects of dielectric shield on the specific absorption rate (SAR) and the temperature increase in the human body exposed to microwave energy. Three shield dielectric properties at microwave frequencies of 300, 915, 1,300, and 2,450 MHz are selected for the shielding investigation. Based on the obtained results, the installed shield strongly affects on the SAR and the temperature increase in human model. The SAR and the temperature increase in human model can be reduced simultaneously by setting the appropriate parameter of the shield (the dielectric properties). The optimum parameter of the dielectric shield greatly depends on the operating frequencies. Additionally, this paper presents an interesting viewpoint on the microwave shielding properties of various dielectric shields. Finally, these fundamental data for the implementations of the radiation protection shielding materials, with focusing on the human organism, are provided as well.

Keywords*:* microwave energy, numerical methods, SAR, heat transfer analysis, dielectric shield.

1. Introduction

As applications of electromagnetic waves become widespread [1, 2], adverse effects caused by the electromagnetic waves are increasingly a subject of concern [3, 4]. In many countries, various studies on biological effects have been made and many results have been reported. There has been intensive model analysis of the SAR of the human body [3, 5, 6]. The protection is serious for researchers who work with high-power electromagnetic waves. In connection with research on human protection from electromagnetic field exposure, some researchers have been carried out on how effectively the human body is protected from unwanted electromagnetic waves [7]. Furthermore, fundamental analysis of shielding effects of lossy dielectric materials located in front of a human body have also been carried out by some researchers [8, 9].

Although the computation of the temperature increase is one of the main tasks in the evaluation of the risk related to the exposure of humans to electromagnetic fields [10], however, most studies of human protection from electromagnetic field exposure do not consider

temperature increase within domain of the human body with complicated layered tissue. There are few studies on the temperature and electromagnetic field interaction in physical model of the human body due to the complexity of the problem, even though it is directly related to the thermal injury of tissues [6, 11, 12]. Therefore, in order to provide information on protection of the human body against electromagnetic fields adequately, it is essential to simulate the coupled electromagnetic field and heat transfer within an anatomically based human body to represent actual process of shield protection from possibly harmful effects of electromagnetic fields.

This paper mainly analyzes the shielding effect of a protective shield being placed in front of a two-dimensional human model. Specifically, lossy dielectric media is chosen as the shield material. The local SARs and temperature increase of human model are calculated for various conditions; operating frequencies, gap distances between shield and human model, and dielectric properties of the dielectric shield. The system of governing equations, as well as initial and boundary conditions are solved numerically, using finite element method (FEM). Moreover, this research is focusing on organs in the human trunk.

2. Formulation of the Problem

As shown in Fig. 1, the incident plane wave E^i (TE wave) with a power density of 5 mW/cm^2 is incident on the shield in front of the human model. A human model including ten kinds of organs was used for our analysis.

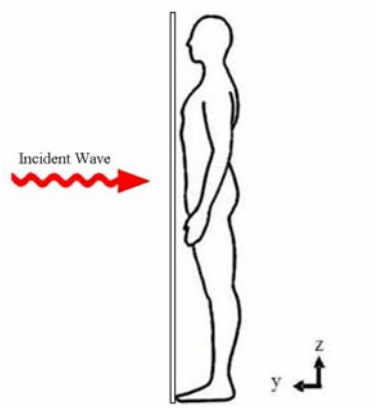

Fig. 1 Human model with dielectric shield

2.1 Human model

From Fig. 2, a human model used in this paper is obtained by image processing technique from the work of Shiba and Higaki [11]. The human model has a dimension of 300 mm in width and 525 mm in height. This human model comprises 10 types of tissue which are skin, bone, muscle, fat, nerve, blood, and so forth. These tissues have different dielectric and thermal properties. The thermal properties and dielectric properties of tissues at the frequencies of 300, 915, 1,300, and 2,450 MHz are given in Table. 1 and Table. 2., respectively. As very few studies associated with human tissue properties have been conducted, some of the tissue properties are not quantified. It is also difficult to directly measure the tissue properties of a live human. Therefore, it should be noted that the properties based on animal experiments are used for most thermal parameters because no actual data is available for analyzing the human model. Fig. 2 shows a vertical cross section through the middle of the human trunk model.

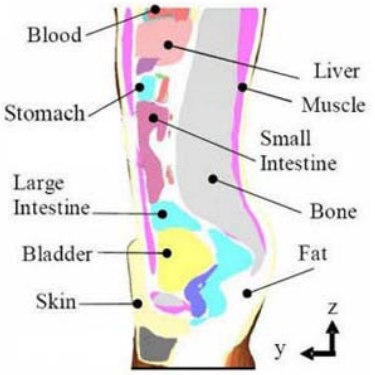

Fig. 2 Human body vertical cross section [11].

Table. 1 Dielectric properties of tissues

Tissue		915 MHz		2,450 MHz	
	ρ (kg/m³)	σ (S/m)	ε_r	σ (S/m)	ε_r
Skin	1,125	0.92	44.86	2.16	41.79
Fat	916	0.09	5.97	0.13	5.51
Muscle	1,047	1.33	50.44	1.60	46.40
Bone	1,038	2.10	44.80	2.10	44.80
Large intestine	1,043	2.04	53.90	2.04	53.90
Small intestine	1,043	3.17	54.40	3.17	54.40
Bladder	1,030	0.69	18.00	0.69	18.00
Blood	1,058	2.54	58.30	2.54	58.30
Stomach	1,050	2.21	62.20	2.21	62.20
Liver	1,030	1.69	43.00	1.69	43.00

Table. 2 Thermal properties of tissues

Tissue	k (W/m·K)	C_p (J/kg·K)	ω_b	Q_{met} (W/m^3)
Skin	0.35	3,437	0.02	1,620
Fat	0.22	2,300	4.58E-04	300
Muscle	0.6	3,500	8.69E-03	480
Bone	0.436	1,300	4.36E-04	610
Large intestine	0.6	3,500	1.39E-02	9,500
Small intestine	0.6	3,500	1.74E-02	9,500
Bladder	0.561	3,900	0.00E+00	
Blood	0.45	3,960		
Stomach	0.527	3,500	7.00E-03	
Liver	0.497	3,600	0.017201	

2.2 Equations for electromagnetic wave propagation analysis

A mathematical model was developed to calculate the electric field and temperature distribution within the human model. To simplify the problem, the following assumptions were made; electromagnetic wave propagation is modeled in two dimensions over the y-z plane, in which waves and object interact proceeds in the open region, and the computational space is truncated by scattering boundary condition. The propagation of an electromagnetic wave is characterized by transverse electric fields (TE-Mode). The dielectric properties of human tissues are temperature and frequency dependent. Since the temperature increase in the human model is slight, the model assumes that the dielectric properties of tissues are constant for the specified frequency.

The electromagnetic wave propagation is calculated by Maxwell's equations [5], which mathematically describe the interdependence of the electromagnetic waves. The general form of Maxwell's equations is simplified to demonstrate the electromagnetic field of microwave penetrated into human model as the following equations:

$$\nabla \times \left(\frac{1}{\mu_r} \nabla \times E \right) - k_0^2 \left(\varepsilon_r - \frac{j\sigma}{\omega \varepsilon_0} \right) E = 0 \qquad (1)$$

$$\varepsilon_r = n^2 \qquad (2)$$

where E is electric field intensity (V/m), μ_r is relative magnetic permeability, n is refractive index, ε_r is relative dielectric constant, $\varepsilon_0 = 8.8542 \times 10^{-12}$ F/m is permittivity of free space, and σ is electric conductivity (S/m), $j = \sqrt{-1}$.

Boundary condition for wave propagation analysis

Microwave energy is emitted by a microwave high power device and strikes the dielectric shield in front of the human model with a particular power density. Therefore, boundary

conditions for electromagnetic wave, as shown in Fig. 3, are considered as follows:

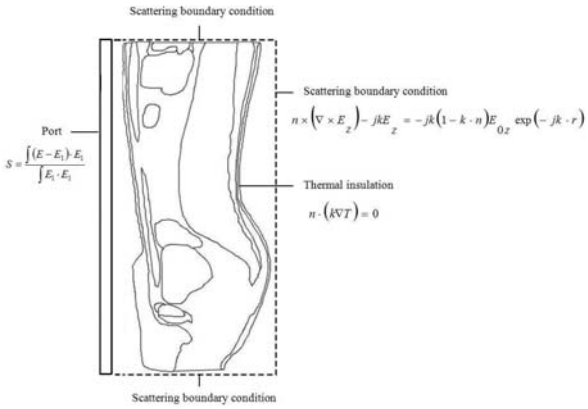

Fig. 3 Boundary condition for analysis

It is assumed that the uniform wave flux strikes the left side of the human model, where the dielectric shield is located. From the viewpoint of convergence of the electromagnetic field, only the TE wave is used as the incident wave. Therefore, at the left boundary of the considered domain, an electromagnetic simulator employs TE wave propagation port with specified power density:

$$S = \int (E - E_1) \cdot E_1 / \int E_1 \cdot E_1 \qquad (3)$$

Boundary conditions along the interfaces between different mediums, for example, between air and tissue or tissue and tissue, are considered as continuity boundary condition:

$$n \times (H_1 - H_2) = 0 \qquad (4)$$

The outer sides of the tissue boundaries are considered as scattering boundary condition:

$$n \times \left(\nabla \times E_z\right) - jkE_z = -jk(1 - k \cdot n)E_{0z} \exp(-jk \cdot r) \qquad (5)$$

2.3 Interaction of electromagnetic waves and human tissues

Interaction of electromagnetic fields with biological tissues can be defined in term of the ***specific absorption rate*** (SAR). Human tissues are generally lossy mediums for EM waves with finite electric conductivity. They are usually neither good dielectric materials nor good conductors. When EM waves propagate through the human tissues, the energy of EM waves is absorbed by the tissues. The specific absorption rate is defined as the power dissipation rate normalized by material density [13]. The specific absorption rate is given by:

$$SAR = \frac{\sigma}{\rho}|E|^2 \qquad (6)$$

where E is the root mean square electric-field (V/m), σ is the conductivity (S/m) and ρ is mass density of the tissue (kg/m^3).

2.4 Equations for heat transfer analysis

Heat transfer analysis of the human model is modeled in two dimensions over the y-z plane. It is assumed that human tissues are bio-material with constant thermal properties. No phase change of substance occurs within the tissues, no energy exchange throughout surface of the human model and no chemical reactions occur within the tissues. There is a continuity boundary condition between the tissue layers within the human model. The temperature distribution inside the human model is obtained by using the Pennes' bio-heat equation [14]. The transient bioheat equation effectively describes how heat transfer occurs within the human model, and the equation can be written as:

$$\rho C \frac{\partial T}{\partial t} + \nabla \cdot (-k\nabla T) = \rho_b C_b \omega_b (T_b - T) + Q_{met} + Q_{ext} \qquad (7)$$

where ρ is the tissue density (kg/m^3), C is the heat capacity of tissue (J/kg·K), k is thermal conductivity of tissue (W/m·K), T is the temperature (°C), T_b is the temperature of blood (°C), ρ_b is the density of blood before entering ablation region (kg/m^3), C_b is the specific heat

capacity of blood (J/ kg·K), ω_b is the blood perfusion rate (1/s), Q_{met} is the metabolism heat source (W/ m^3) and Q_{ext} is the external heat source (microwave heat-source density) (W/ m^3).

In the analysis, heat conduction between tissue and blood flow is approximated by the term $\rho_b C_b \omega_b (T_b - T)$. The thermoregulation mechanisms and the metabolic heat generation of each tissue have been neglected to illustrate the clear temperature distribution.

The external heat source is equal to the resistive heat generated by electromagnetic field (microwave power absorbed term)

$$Q_{ext} = \frac{1}{2}\sigma_{tissue}\left|\overline{E}\right|^2 \quad (8)$$

Boundary condition for heat transfer analysis

The heat transfer analysis is considered only in the human model domain, which does not include parts of the surrounding space and dielectric shield. At the skin–air interface, the insulated boundary condition has been imposed to clearly illustrate the temperature increase. As shown in Fig. 3, the surfaces of human model are considered as insulated boundary condition:

$$n.(k\nabla T) = 0 \quad (9)$$

It is assumed that no contact resistant occurs between the internal layers of the human model. Therefore, the internal boundaries are assumed to be a continuity boundary condition:

$$n \cdot (k_u \nabla T_u - k_d \nabla T_d) = 0 \quad (10)$$

Initial condition for heat transfer analysis

For this analysis, the temperature distribution within human model is assumed to be uniform and kept constant throughout the human model, which defined as:

$$T(t_0) = 37\,^{\circ}\mathrm{C} \quad (11)$$

3. Results and Discussion

In this section, a dielectric shield is placed in front of the human model in order to provide information on protection of the human against electromagnetic radiation. Different dielectric properties of dielectric shield for electromagnetic wave protection effectiveness are also analyzed by using the FEM method in conjunction with a detailed human model.

Fig. 4 shows the initial meshes of the human model as well as the SAR and temperature distribution in the human model exposed to the power density of 5mW/cm^2 at the frequency of 300MHz.

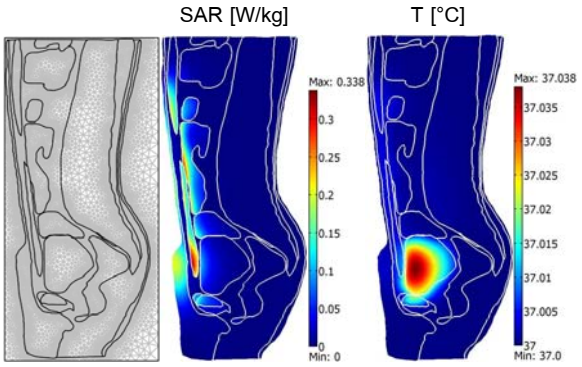

(a) (b) (c)

Fig. 4 The finite element analysis of the human model exposed to the microwave power density of 5mW/cm^2 at the frequency of 300MHz

a. An initial finite element meshes of human cross section model.

b. SAR distribution of the shieldless case.

c. Temperature distribution of the shieldless case.

The effects of the operating frequency on shielding effect of dielectric shield are investigated. The relative permittivity values for the shield are chosen as (low-loss; 10-*j*5), (medium-loss; 10-*j*10), and (high-loss; 20-*j*20). Fig. 5 and Fig. 6 show the maximum SAR and maximum temperature increase in human model

at the frequencies of 300MHz, 915MHz, 1,300MHz and 2,450MHz. The shield gap distance is set to 0.5cm and shield thickness to 0.3cm.

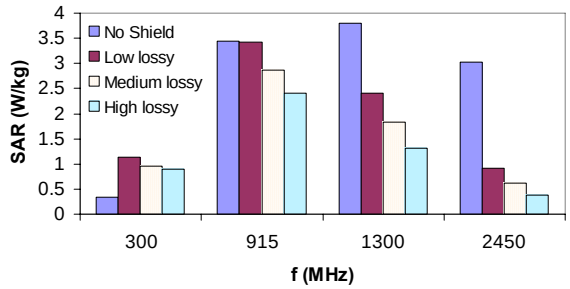

Fig. 5 Comparison of the maximum SAR in human model at the frequencies of 300MHz, 915 MHz, 1,300MHz and 2,450 MHz

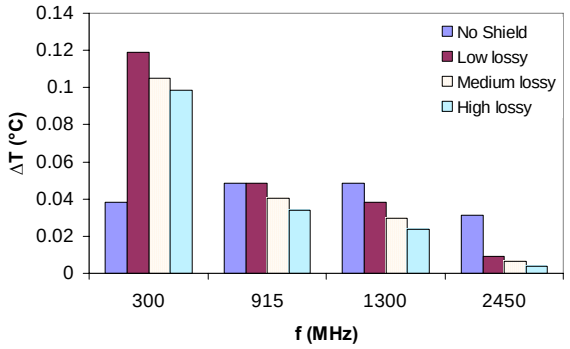

Fig. 6 Comparison of the maximum temperature increases in human model at the frequencies of 300MHz, 915 MHz, 1,300MHz and 2,450 MHz

It is evident from Fig. 5 and Fig. 6 that the frequency ranges of 1,300 and 2,450 MHz, a significant reduction of SAR and temperature increase within human model are achieved. However, in the frequency range of 300MHz, the SAR and the temperature increase varied greatly and increased compared to the unshielded value. This is because of the multiple reflections between the gaps caused the accumulation of microwave energy in the gap and increased the SAR and temperature increase.

Due to the layer resonance within human model, the unshielded maximum SAR increase from 300 MHz and the maximum value appeared at 1,300 MHz as shown in Fig. 5, while the unshielded maximum temperature increase appeared at 915MHz as shown in Fig. 6. This is because of the different of dielectric and thermal properties of tissues.

Based on the results of the local SAR of the unshielded human model, at a low frequency of 300 MHz, large value of SAR are occurred, found at the small intestine and muscle layers. With the use of the low lossy shield, the greater values of SAR are occurred compare to the unshielded human model as shown in Fig. 7.

At a high frequency of 2,450 MHz, a large value of local SAR is found at the skin layer. However, large reduction of the SAR value is achieved when using the same dielectric shield (low-loss shield) with the frequency of 300 MHz as shown in Fig. 8.

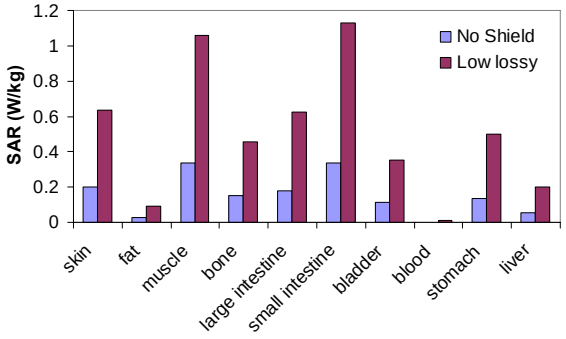

Fig. 7 Comparison of the maximum SAR in human organs of the unshielded and shielded human model at the frequency of 300 MHz

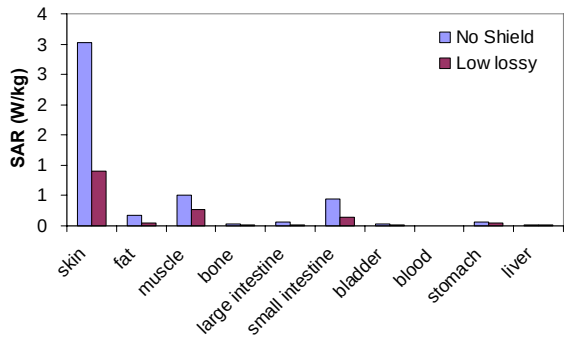

Fig. 8 Comparison of the maximum SAR in human organs of the unshielded and shielded human model at the frequency of 2,450 MHz

The obtained results in Fig. 7 and Fig. 8 show that the maximum SAR and the maximum temperature increase in human model primarily depends on the penetration depth of microwave power which correspond to the operating frequency as well as dielectric properties of dielectric shield.

On placing the low lossy shield in front of the human model, in the frequency of 300 MHz, the maximum SAR value varied greatly and increased compared to the unshielded value.

As the dielectric properties of a dielectric shield vary, the penetration depth will be changed and the electric field passing through the dielectric shield is altered. If the penetration depth is changing, a fraction of the incident energy absorbed is also changed.

4. Conclusion

This paper presents the simulations of specific absorption rate and heat transfer in the human model, which is protected from microwave energy by a dielectric shield. The specific absorption rate and temperature distributions in the human model are governed by the electric field as well as dielectric properties of tissue.

The results show an interaction between physical parameters; operating frequencies and shield dielectric properties. It is evident from the results that the frequency ranges of 1,300 and 2,450 MHz, a significant reduction of SAR and temperature increase within human model are achieved. However, in the frequency range of 300MHz, the SAR and the temperature increase varied greatly and increased compared to the unshielded value.

Due to the layer resonance within human model, the unshielded maximum SAR increased from 300 MHz and the maximum value appeared at 1,300 MHz, while the unshielded maximum temperature increase appeared at 915MHz. This is because of the different of dielectric and thermal properties of tissues.

Future work will include the calculations of the SAR and the temperature increase for a three-dimensional model. It will be necessary in the future to study the cases of different frequencies and of TM waves. Moreover, it is necessary to research the effects of the shield not only in the case of the plane wave, but also in the case of the near field. Calculations of the SAR and the temperature increase for a more realistic situation should be carried out.

5. Acknowledgement

The authors gratefully acknowledge the financial support provided by The Thailand Research Fund (TRF) for the simulation facilities described in this paper.

6. References

[1] P. Rattanadecho, N. Suwannapum, A. Watanasungsuit, and A. Duanduen, "Drying of dielectric materials using a continuous microwave belt drier (Case study: Ceramics and natural rubber)," *Journal of Manufacturing Science and Engineering, Transactions of the ASME,* vol. 129, pp. 157-163, 2007.

[2] P. Ratanadecho, K. Aoki, and M. Akahori, "The characteristics of microwave melting of frozen packed beds using a rectangular waveguide," *IEEE Transactions on Microwave Theory and Techniques,* vol. 50, pp. 1495-1502, 2002.

[3] M. A. Stuchly, "Health effects of exposure to electromagnetic fields," in *IEEE Aerospace Applications Conference Proceedings*, 1995, pp. 351-368.

[4] K. L. Ryan, J. A. D'Andrea, J. R. Jauchem, and P. A. Mason, "Radio frequency radiation of millimeter wave length: Potential occupational safety issues relating to surface heating," *Health Physics,* vol. 78, pp. 170-181, 2000.

[5] R. J. SPIEGEL, "A Review of Numerical Models for Predicting the Energy Deposition and Resultant Thermal Response of Humans Exposed to Electromagnetic Fields," *IEEE TRANSACTIONS ON MICROWAVE THEORY AND TECHNIQUES,,* vol. MTT-32, pp. 730-746, 1984.

[6] A. Hirata, T. Fujino, and T. Shiozawa, "SAR and temperature increase induced in the human body due to body-mounted antennas," in *Antennas and Propagation Society International Symposium, 2004. IEEE*, 2004, pp. 1851-1854 Vol.2.

[7] A. W. Guy, C.-K. Chou, J. A. McDougall, and C. Sorensen, "MEASUREMENT OF SHIELDING EFFECTIVENESS OF MICROWAVE-PROTECTIVE SUITS," *IEEE Transactions on Microwave Theory and Techniques,* vol. MTT-35, pp. 984-994, 1987.

[8] S. Nishizawa and O. Hashimoto, "Effectiveness analysis of lossy dielectric shields for a three-layered human model," *IEEE Transactions on Microwave Theory and Techniques,* vol. 47, pp. 277-283, 1999.

[9] O. Hashimoto and S. Nishizawa, "Effectiveness analysis of thin resistive sheet for a three-layered elliptical human model," *Microwave and Optical Technology Letters,* vol. 23, pp. 73-75, 1999.

[10] T. Samaras, A. Christ, A. Klingenbรถck, and N. Kuster, "Worst case temperature rise in a one-dimensional tissue model exposed to radiofrequency radiation," *IEEE Transactions on Biomedical Engineering,* vol. 54, pp. 492-496, 2007.

[11] K. Shiba and N. Higaki, "Analysis of SAR and current density in human tissue surrounding an energy transmitting coil for a wireless capsule endoscope," in *Proceedings of the 20th International Zurich Symposium on Electromagnetic Compatibility, EMC Zurich 2009*, Zurich, 2009, pp. 321-324.

[12] A. Hirata, O. Fujiwara, and T. Shiozawa, "Correlation Between Peak Spatial-Average SAR and Temperature Increase Due to Antennas Attached to Human Trunk," *Biomedical Engineering, IEEE Transactions on,* vol. 53, pp. 1658-1664, 2006.

[13] A. Hirata, M. Fujimoto, T. Asano, J. Wang, O. Fujiwara, and T. Shiozawa, "Correlation

between maximum temperature increase and peak SAR with different average schemes and masses," *IEEE Transactions on Electromagnetic Compatibility,* vol. 48, pp. 569-577, 2006.

[14] D. Yang, M. C. Converse, D. M. Mahvi, and J. G. Webster, "Expanding the bioheat equation to include tissue internal water evaporation during heating," *IEEE Transactions on Biomedical Engineering,* vol. 54, pp. 1382-1388, 2007.

[15] P. Ratanadecho, K. Aoki, and M. Akahori, "A numerical and experimental investigation of the modeling of microwave heating for liquid layers using a rectangular wave guide (effects of natural convection and dielectric properties)," *Applied Mathematical Modelling,* vol. 26, pp. 449-472, 2002.

[16] P. Ratanadecho, K. Aoki, and M. Akahori, "Influence of irradiation time, particle sizes, and initial moisture content during microwave drying of multi-layered capillary porous materials," *Journal of Heat Transfer,* vol. 124, pp. 151-161, 2002.